Available online at www.sciencedirect.com
ScienceDirect
Food Chemistry 107 (2008) 305–311
Food Chemistry
www.elsevier.com/locate/foodchem

Investigation of chemical structure of nonprotein proteinase inhibitors from dried figs

Ken-ichi Hatano [a,*], Kenji Kubota [a], Masaru Tanokura [b]

[a] Department of Biological Sciences, Faculty of Engineering, Gunma University, 1-5-1 Tenjin-cho, Kiryu, Gunma 376-8515, Japan
[b] Department of Applied Biological Chemistry, Graduate School of Agricultural and Life Sciences, The University of Tokyo, 1-1-1 Yayoi, Bunkyo-ku, Tokyo 113-8657, Japan

Received 23 October 2006; received in revised form 7 August 2007; accepted 7 August 2007

Abstract

Two types of the nonprotein proteinase inhibitors, P and B samples were previously isolated from dried figs by gel permeation and high-performance liquid chromatography. In the present study, we investigated the chemical structure of the B sample using both mass spectrometry (MS) and solid-state nuclear magnetic resonance. Fast atom bombardment and matrix-assisted laser desorption ionization-time of flight MS experiments showed losses of 16, 44, 176, and 338 Da. By electrospray ionization tandem MS, the product-ion spectra of *m/z* 712, 731, and 750 in the parent ions indicated that the fragmentation ion at *m/z* 175 was the repeated structure of the parent ions. We propose here that the 176- and 338-Da compounds might aggregate each other, probably by polymerizations, ether linkages, and hydrogen bonding, which would result in a mass variety of the B sample as observed in the MS analyses.

Keywords: *Ficus carica*; Humic substances; Organic matter; Nonprotein; Chemical structure; Proteinase inhibitor

1. Introduction

The fig tree (*Ficus carica*) is cultivated for its fruit in temperate zones, and the dried fruit has been a food familiar to human beings since B.C. 3000. Nutritionally, dried figs provide a high quantity of calcium, potassium, and dietary fiber as compared with any other common fruit (Vinson, Zubik, Bose, Samman, & Proch, 2005); in addition, human beings have taken them as a laxative, an expectorant, and a hemorrhoidal drug since ancient times. Recently, Hatano has found that dried figs possess weak inhibitory activities against some proteinases, and the relationship between their effects as a laxative and the inhibitory activities have become a point of interest. In a previous study (Hatano, 2006), he purified the inhibitory components, P and B samples, from dried figs, measured their inhibitory activities against some digestive enzymes, and briefly characterized their molecular structures. The inhibitory components were revealed to inhibit a ficin-like proteinase papain as well as a digestive enzyme chymotrypsin. The UV–Vis and infrared absorption (IR) spectra indicated that they might be a kind of humic substances, the environmental degradation products of plant, fungal, and bacterial biopolymers. Humic substances are divided into three operationally defined fractions: humine, which is insoluble in aqueous solution at all pH values; humic acid, which is soluble only in alkaline aqueous solution; and fulvic acid, which is soluble in aqueous solution at any pH value.

Elemental analysis, ^{13}C nuclear magnetic resonance (NMR), and IR spectrometry have been used to evaluate the chemical structure such as humic substances. These methods, however, do not give definite information about specific components but instead describe an 'average' characteristic of the bulk material. In recent years, electrospray ionization (ESI) mass spectrometry (MS) has provided considerable progress in the characterization and analysis

* Corresponding author. Tel./fax: +81 277 30 1401.
E-mail address: hatano@chem-bio.gunma-u.ac.jp (K.-i. Hatano).

0308-8146/$ - see front matter © 2007 Elsevier Ltd. All rights reserved.
doi:10.1016/j.foodchem.2007.08.029

of fulvic acid, since this technique makes intact molecules accessible to MS. Structural regularities have been determined in the product-ion spectra of fulvic acid by ESI tandem MS (ESI-MS/MS) technique as well as in the spectra by ESI-MS (Plancque, Amekraz, Moulin, Toulhoat, & Moulin, 2001). On comparing the various spectra, it appears that fulvic acids from very different origins exhibit very similar molecular mass patterns and nearly identical fragmentation behavior (Reemtsma & These, 2003). These various studies using ESI-MS indicated that fulvic acid is not a mixture of a virtually indefinite number of unique molecules. Previously, Hatano measured the preliminary spectra of the P and B samples using matrix-assisted laser desorption ionization-time-of-flight MS (MALDI-TOF-MS). He demonstrated that these samples consist of relatively small molecules with molecular masses around 500–1400 Da, although the detailed chemical and conformational structure could not be determined (Hatano, 2006).

In this paper, we focused on the B sample due to its high ionization efficiency and chose several MS techniques to obtain insight into the structural regularities as observed in the fulvic acids. On the other hand, we worry that the MS data may only provide the structural information derived from the ionized sample. Therefore, we combined the MS data with the data of solid-state NMR and elemental analysis that provide us with information regarding both the ionized and unionized sample. As a result, the regularities of molecular mass patterns were observed on the MS spectra of the B sample. However, the elemental analysis and solid-state NMR spectra showed that the sample was not the typical humic materials, fulvic acid and humic acid, indicating that this sample is a novel organic matter. At last, based on the above-mentioned data, we propose the putative chemical structure of the B sample.

2. Materials and methods

2.1. Materials

Dried fig fruit in California (Black Mission) was purchased from a local market, and the P and B samples were purified as described previously (Hatano, 2006). Stock solutions of the samples for MS analysis were prepared in Milli-Q water at a concentration of 1 mg/mL. 2,5-Dihydroxybenzoic acid (DHB) was purchased from Sigma–Aldrich (St. Louis, MO). All other reagents used were of the highest grade commercially available.

2.2. Elemental analysis

The samples were characterized for their carbon and nitrogen content using a Sumigraph model-NC22 (Sumika Chemical Analysis Service, Tokyo, Japan). The carbon and nitrogen content was obtained by burning 3.0 mg of each sample in reactor and reduction ovens at 830 and 600 °C, respectively. Acetanilide was used as a calibration standard ($N = 10.36\%$ and $C = 71.09\%$).

2.3. Solid-state NMR spectroscopy

All NMR experiments were carried out with a Varian Unity INOVA 400WB spectrometer (Varian Technologies, Tokyo, Japan) operating at resonance frequencies of 399.847 MHz for ^{1}H and 100.559 MHz for ^{13}C. One hundred milligrams of each sample were packed into 7-mm zirconia rotors and placed in the spinning module of a Jakobsen cross polarization/magic angle spinning (CP/MAS) probe. CP was achieved with variable-amplitude spin-lock fields (Peersen, Wu, Kustanovich, & Smith, 1993). The typical 90° pulse length for ^{13}C was 3.1 μs, and a CP contact time of 4 ms was used to minimize background signals. The ^{1}H radio frequency field strength for heteronuclear two-pulse phase modulation decoupling was approximately 72 kHz (Bennett, Rienstra, Auger, Lakshmi, & Griffin, 1995). Typical recycling delays were 5 s, and acquisition times were 80 ms. ^{13}C and ^{1}H chemical shifts were referenced externally to tetramethylsilane through adamantane and water, respectively. Sample spinning speeds were regulated to 5208 Hz using a Varian pneumatic control unit. The digital resolution (DR) was calculated by the following equation:

$$\mathrm{DR} = 2 \times \mathrm{SW}/\mathrm{FN} = 2 \times 50\mathrm{k}/16\mathrm{k} = 6.3\ \mathrm{Hz/point}$$

where SW is the spectral width, and FN means data points after Fourier transformation.

The conventional ^{1}H–^{13}C heteronuclear correlation (HETCOR) experiment was carried out, based on the sequence of Bielecki and coworkers (Bielecki, Burum, Rice, & Karasz, 1991). Typical radio frequency pulse lengths were 4.0 μs for ^{13}C and ^{1}H. Multiple-pulse ^{1}H decoupling (BLEW-12) was applied during evolution to suppress ^{1}H–^{1}H homonuclear interactions. Additional multiple-pulse ^{13}C irradiation (BB-12) was performed synchronously with BLEW-12 to suppress ^{1}H–^{13}C dipolar interactions. Following the evolution period, the ^{1}H intensity was selectively transferred to carbon with a single cycle of the multiple-pulse sequence WIM-24, which causes cross-polarization while effectively suppressing ^{1}H spin diffusion. In case of the P sample, the DR was $2 \times 50\mathrm{k}/4\mathrm{k} = 25$ Hz/point in the f_2 dimension and $2 \times 10\mathrm{k}/4\mathrm{k} = 5$ Hz/point in the f_1 dimension; on the other hand, that of the sample B was $2 \times 50\mathrm{k}/8\mathrm{k} = 12.5$ Hz/point in the f_2 dimension and $2 \times 10\mathrm{k}/4\mathrm{k} = 5$ Hz/point in the f_1 dimension. The other conditions were the same as those for the CP/MAS experiments.

2.4. Mass spectrometry

FAB-MS was carried out on a JEOL JMS-SX102 spectrometer (JEOL, Tokyo, Japan) for the initial characterization. Thioglycerol and 1-N hydrochloric acid were added to the stock solution in a volume ratio of 5:1. The JMS-

SX102 has a mass range of 3500 Da at 8-kV accelerating potential, and approximately 0.5–0.7 μL of the thioglycerol matrix containing the sample was applied to a stainless steel sample stage mounted on the end of a high-vacuum push rod.

MALDI-TOF-MS analysis was performed on a KOMPACT MALDI-4 mass spectrometer (Shimadzu/Kratos, Manchester, UK). A DHB matrix-saturated solution was prepared in a 3:7 mixture of acetonitrile and Milli-Q water containing 0.1% trifluoroacetic acid. The dried-droplet technique was used for MALDI-TOF-MS sample preparation. The mass spectra were recorded on both linear and reflection modes, and the mass range was m/z 0–3000.

MS/MS experiments were conducted using a Q-TOF-II mass spectrometer (JASCO International/Micromass, Manchester, UK) equipped with a Nanoflow ESI interface. Sample solutions were prepared by 10-fold dilution of the stock solutions in methanol/0.28% ammonia (1:1) and introduced into a Nanoflow capillary with a flow rate set to 10–50 nL/min. The capillary needle voltage was set at 1–1.5 kV. The best conditions were: source temperature 80 °C, cone voltage 50 V, and collision energy 25 eV.

We were not able to obtain the MALDI-TOF and ESI-Q-TOF mass spectra of the P sample with good quality, which would be due to the low ionization efficiency (Hatano, 2006).

3. Results and discussion

3.1. Elemental analysis

The carbon and nitrogen content of the B sample showed $34.3 \pm 0.1\%$ and $6.5 \pm 0.0\%$, respectively. On the other hand, the elemental analysis of the P sample is reported $40.9 \pm 0.1\%$ for carbon and $1.5 \pm 0.0\%$ for nitrogen. In general, the carbon and nitrogen content of typical fulvic acids (humic acids) from ground water, river, and sea indicates 51.0–59.7% (50.5–62.1%) and 0.7–1.1% (0.6–3.2%), respectively (Thurman, 1985). Obviously, the carbon content of the organic matter from dried figs, especially the B sample, was lower than that of the fulvic and humic acids; therefore, it seems that the chemical structure of the B sample is considerably different from that of the humic materials.

Only the analysis of carbon and nitrogen can be performed with the Sumigraph model-NC22. Accordingly, we calculated only the C/N ratio and revealed that the ratios of the samples P and B were 27.3 and 5.3, respectively. Generally, it is believed that the C/N ratios of humic acid, rice straw, legume, and microbial origin are 15–25, 60, 20–30, and 4–9, respectively (Thurman, 1985). The ratio of the B sample therefore indicates that this novel substance is likely from microbial origin. There could be humic acid from microbial origin, but here the B sample showed the lower carbon content, indicating that this sample is not humic acid.

3.2. Solid-state NMR spectra

Plates A and B of Fig. 1 display the ^{13}C-CP/MAS NMR spectra of the B and P samples from dried figs, respectively. The CP/MAS spectrum of the B sample was dominated by two sharp signals at 61.6 and 57.5 ppm, and that of the P sample showed several broad resonances around 171.7, 131.2, 121.1, 104.1, 79.3, 70.0, and 18.3 ppm. These resonances were assigned to nonpolar carbon atoms such as the aromatic/olefin (160–110 ppm) and aliphatic carbons (45–0 ppm), and to polar carbon atoms such as the carboxyl/carbonyl (190–160 ppm), C–O and C–N groups, and anomeric carbons (110–45 ppm). The spectral pattern of the P sample was similar to that of fulvic and humic acids from the Suwannee River; however, the intensities of the peak regions of >100 ppm and <50 ppm were much lower than the intensities in the fulvic and humic acids (Thurman, 1985). The spectral pattern of the B sample was simple and quite different from that of the fulvic and humic acids, indicating that the chemical structure of the B sample is different from that of the humic matters.

The ^{1}H–^{13}C HETCOR spectra of the B and P samples are shown in Fig. 1C and D, respectively. Four cross peaks (a–d) were visible in the spectrum of the B sample, while there were six cross peaks (a–f) in that of the P sample. Interestingly, the carbon resonance at 57 ppm in Fig. 1C gave three cross peaks in the ^{1}H dimension (b–d peaks), indicating that hydrogens bonded to the carbon exist in three different environments. Especially, the proton resonance at 12.2 ppm (peak d) suggests that this proton would form a strong hydrogen bond, since proton NMR chemical shifts have significant correlation with the length of hydrogen bonds (Wagner, Pardi, & Wüthrich, 1983). Similarly, in case of the P sample, three cross peaks in the ^{1}H dimension (b–d peaks) were observed in the resonance at 70 ppm for carbon (Fig. 1D). As is seen, the NMR spectra of the B sample revealed very simple and this sample appears to be suitable for further structural analysis.

3.3. FAB and MALDI-TOF mass spectra

The FAB-MS spectra of the P and B samples in a positive ion mode were very similar to each other (data not shown), although the signal-to-noise ratio (S/N) was relatively poor. The mass-distribution shapes of the B sample indicated a shifted sinebell function with a periodicity of 44 Da, and the maximum molecular weight of the B sample was estimated approximately 1500 Da (data not shown). We call the fragment of 44-Da a *quark* (Q) module for an explanation of the fragmentation scheme.

Fig. 2A illustrates the MALDI-TOF mass spectrum of the sample B on a linear mode. The spectrum showed obvious regularities in peak appearance, as indicated in Table 1. There were two peak-appearance groups (higher peaks at m/z 361, 699, 1037, and 1375; lower ones at m/z 537, 875, 1213, and 1566). The mass difference between the two groups (for example, peaks at m/z 361 and 537)

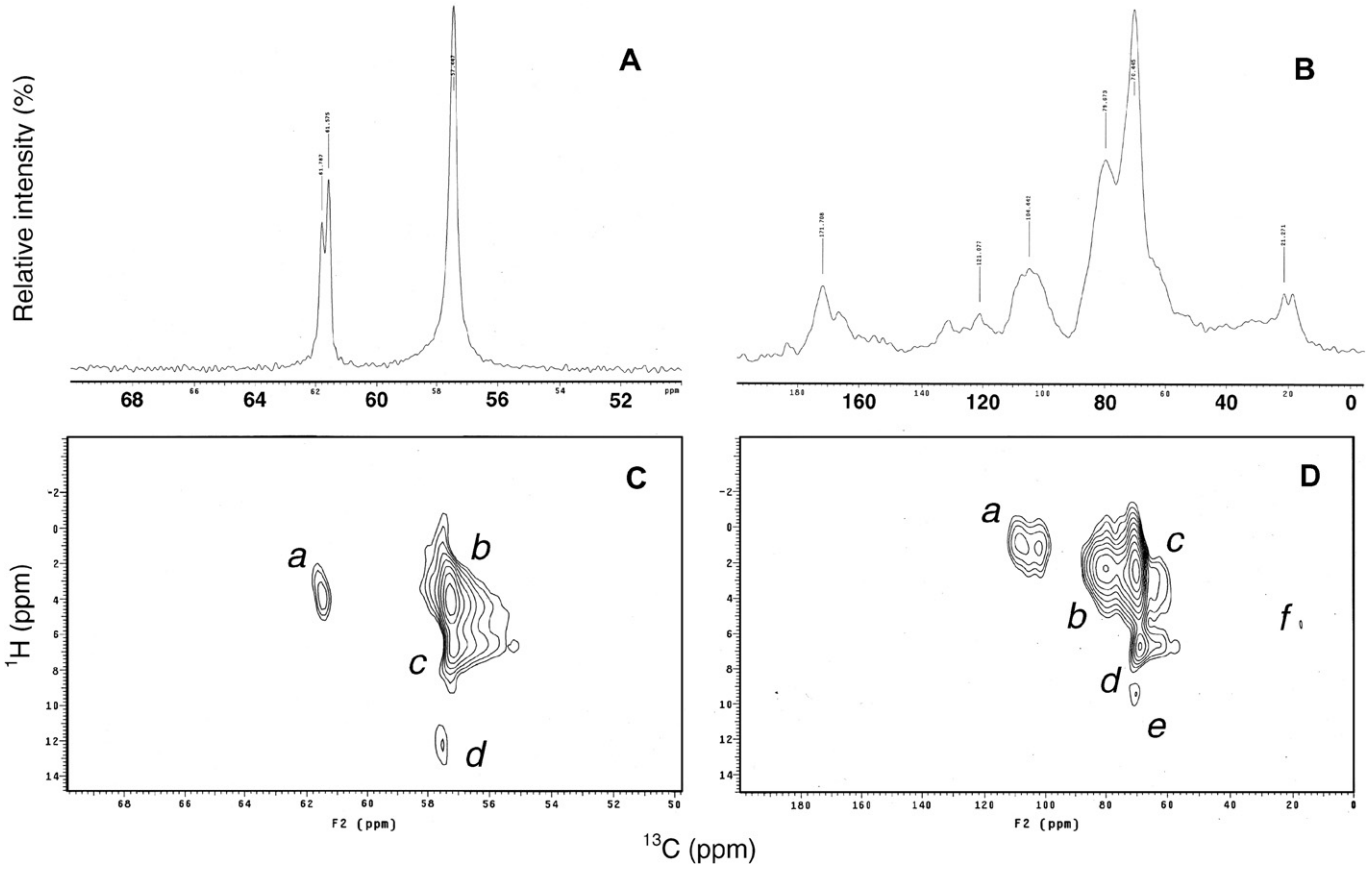

Fig. 1. Solid-state NMR spectra of the B and P samples from dried figs. The ^{13}C-CP/MAS spectra of the B and P samples are shown in (A) and (B), respectively. Plates C and D indicate the 2D ^{13}C–^{1}H HETCOR spectra of the samples B and P, respectively. Carbon chemical shifts are referenced to adamantane and are accurate to ±0.05 ppm.

certainly indicated 176 Da, while the differences among the peaks within each group (for instance, peaks at *m/z* 361 and 699) were 338 Da (Table 1). Here, we respectively designate the fragments of 176 and 338 Da *atom* modules, A1 and A2. Each peak had some additional peaks, probably the precursor ions $[M-O]^+$ and $[O-M-O]^+$ (Table 1), indicating that each precursor ion has two ether-linkage sites.

Fig. 2B shows the post-source decay (PSD) spectrum of the B sample on a reflection mode. The most intense product ion at *m/z* 361 would probably be a starting material for the polymerization of the B sample, since sample fragmentations in the source region are strongly induced in the PSD experiments. The product ions at *m/z* 355, 361, and 377 would be the oxygen and sodium adduct of the A2 module, probably $[A2-O]^+$, $[A2-Na]^+$, and $[O-A2-Na]^+$, respectively (Table 1). Actually, sodium ions were detected as a peak at *m/z* 23 in the spectrum (Fig. 2B).

3.4. ESI-Q-TOF tandem mass spectra

The ESI-Q-TOF mass spectrum and the zoomed one (*m/z* 600–900) of the sample B are shown in Fig. 3A and the inset, respectively. Two mass distributions (*m/z* 100–400 and 1000–1500) indicated monovalent anions with 1.0-Da inter-peak spacing (Fig. 3A); in contract, the distribution in the range between *m/z* 600–900 showed divalent anions that were observed at every half-mass (Fig. 3A, inset). We observed three peak clusters at the beginning *m/z* 624, 712, and 800 in the enlarged spectrum, each of which would have two binding sites such as $[M-K]^-$ and $[K-M-K]^-$ (Table 2). The mass difference between the three clusters appeared to be 88 Da, which corresponded to singly charged ions at *m/z* 176 (Table 2).

Fig. 3B–D shows the product-ion spectra of *m/z* 712, 731, and 750 (intense signals in the inset of Fig. 3A), respectively. The fragmentation ion at *m/z* 175 was the most intense among the other peaks and was considered as a representative repeated structure of the parent ions (Table 2). Accordingly, these product ions would be assembled by a number of the A1 modules. We also observed the other important fragments of 113, 131, 193, and 351 Da in Fig. 3B–D, indicating elimination of water from three Q modules, three Q modules, the addition of water to the A1 module, and two A1 modules, respectively (Table 2). Thus, we could explain the constitution of all the product ions using the Q module, which is consistent with the results of the FAB-MS experiment.

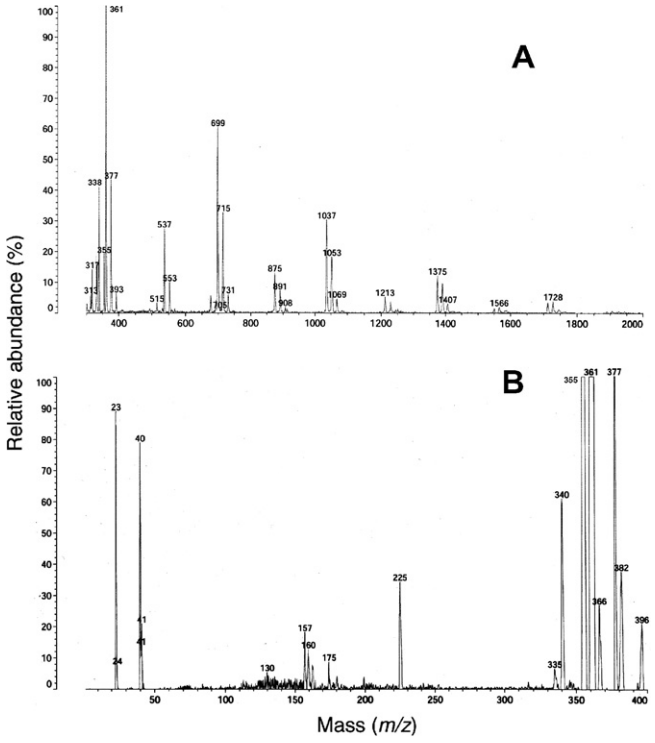

Fig. 2. MALDI-TOF mass spectra of the B sample: (A) normal spectrum on a linear mode; (B) post-source decay spectrum on a reflection mode.

Table 1
MALDI-TOF mass spectra of the B sample at m/z 300–1100

Experimental mass (m/z)	Mass gain (Da)	Relative intensity (%)	Assigned fragment
Normal spectrum			
338	338	41	A2 [=113 × 3]
361	338, 23	100	A2(Na)
377	361, 16	44	A2(O)
393	361, 16 × 2	6	A2(O,O)
537	361, 176	27	A1 + A2(Na)
553	361, 176, 16	10	A1 + A2(Na,O)
699	361, 338	60	A2 + A2(Na)
715	361, 338, 16	33	A2 + A2(Na,O)
731	361, 338, 16 × 2	7	A2 + A2(Na,O,O)
875	361, 338, 176	14	A1 + A2 + A2(Na)
891	361, 338, 176, 16	8	A1 + A2 + A2(Na,O)
908	361, 338, 176, 16 × 2	2	A1 + A2 + A2(Na,O,O)
1037	361, 338 × 2	30	$(A2)_2$ + A2(Na)
1053	361, 338 × 2, 16	18	$(A2)_2$ + A2(Na,O)
1069	361, 338 × 2, 16 × 2	6	$(A2)_2$ + A2(Na,O,O)
PSD spectrum			
355	338, 16	70	A2(O)
361	338, 23	100	A2(Na)
377	338, 23, 16	15	A2(Na,O)

3.5. Putative molecular structure

Humic materials have the ability to form rather stable complexes cations, probably carboxylic and phenolic groups as the main complex functionalities (Aiken, McKnight, Wershaw, & MacCarthy, 1985; Hayes, MacCarthy, Malcolm, & Swift, 1989; Stevenson, 1985). For instance, Plancque et al. (2001) discovered the existence of product ions at m/z 133, 177, and 371 by the ESI-Q-TOF-MS experiments of groundwater fulvic acid. Similarly, Leenheer and coauthors (2001) demonstrated the chemical structure of product ion at m/z 329 from fulvic acid from the Suwannee River. In this work, we were able to observe product ions at m/z 131 and 176 in the B sample, and the solid-state NMR study revealed that this sample contained neither carboxyl/carbonyl groups nor aromatic/olefin (Fig. 1A). Therefore, we concluded that the B sample is not these humic substances, not only because the sample has neither carboxyl nor aromatic nor olefin, but also because the sample has a C/N ratio that is less than half of the minimum reported for the substances. On the other hand, dried figs contain a large amount of sugar, some of which appeared to be condensed and dehydrated. Considering that the color of the B sample is brown, the sample might be produced by the typical browning reaction in foods, the Maillard reaction or sugar caramelization. However, we could not detect the representative ^{13}C NMR signals (140 and 110 ppm) of the main product from these reactions, furfural derivatives (Fig. 1A).

We propose here the fragmentation scheme of the sample B, which allows us to predict the preliminary molecular structure (Q module) as follows:

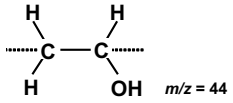

The sample would be composed of the modules A1 and A2, each of which is made of the Q module. The A1 module would be formed by polymerization of four Q modules (Fig. 4A and B), while the module A2 might be formed by trimerization of the dehydrated polymer from three Q modules (Fig. 4C). The modules A1 and A2 might connect with each other, probably by polymerizations, ether linkages, and hydrogen bonding, leading to a mass variety of the B sample (designed as a *molecular* module) as observed in the MS spectra. For example, the precursor ion of 891 Da, one of the molecular (M) module, might be composed of one A1 module and two A2 modules, one of which is the sodium and oxygen adduct (Table 2). Thus, we could explain almost all M modules of the sample B using the modules Q, A1, and A2. However, we must remember that these product ions were observed just by ionization of the MS experiments. In this scheme, we do not address the large amounts of nitrogen observed in the elemental analysis. Probably, the nitrogen atoms would constitute a part of the unionized moiety, which might be involved in hydrogen bonding like O–H···N. Similarly, the P sample would be composed of the Q module

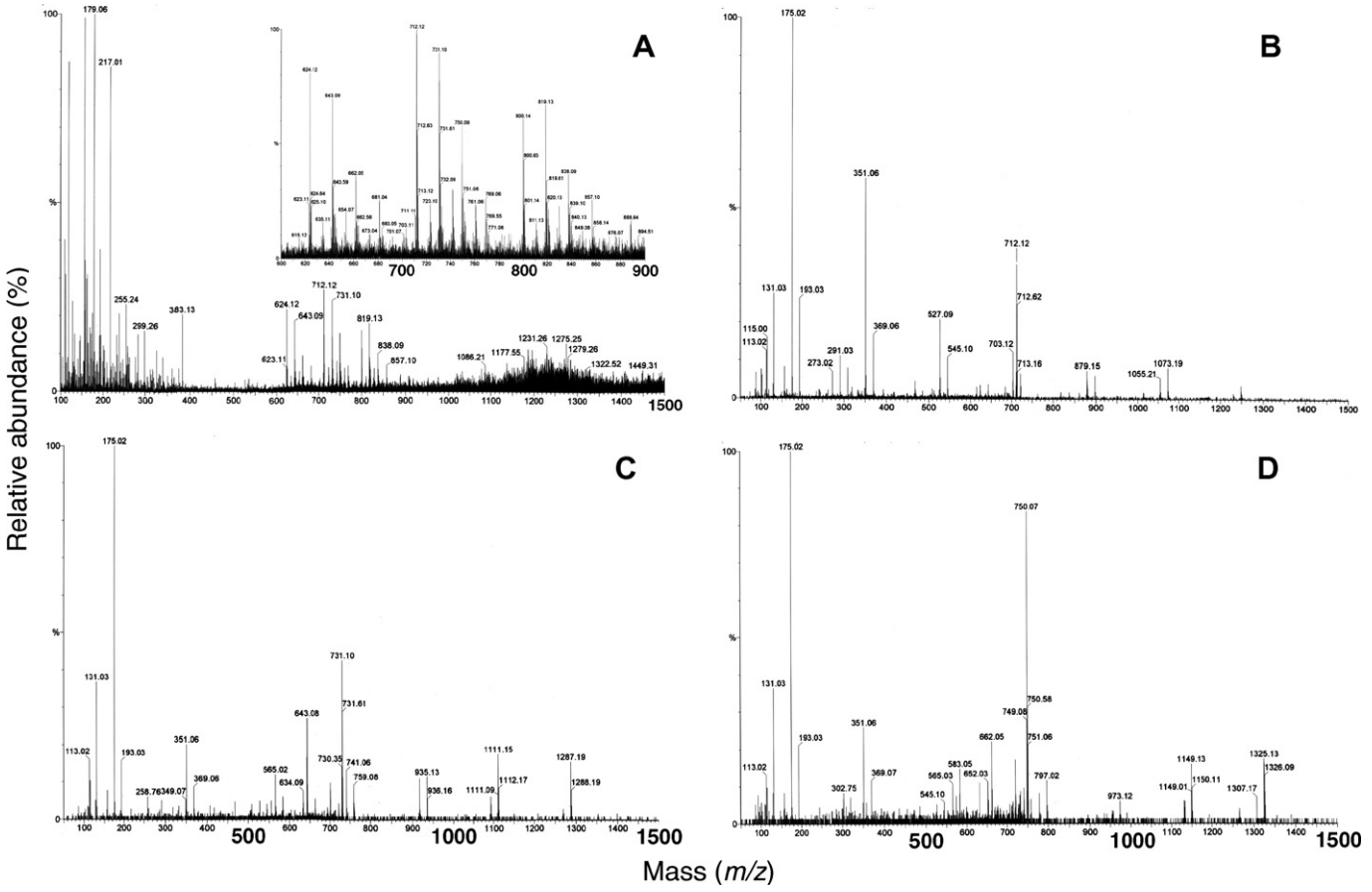

Fig. 3. Negative-ion ESI mass spectra of the B sample acquired under optimized conditions (A) and the product ion spectra obtained by ESI MS/MS of the selected anions of *m/z* 712 (B), 731 (C), and 750 (D).

Table 2
ESI-MS/MS spectra of the negative precursor ion at *m/z* 712, 731, and 750 in the B sample

Experimental mass (*m/z*)	Mass gain (Da)	Relative intensity (%)	Assigned fragment
Precursor-ion peaks (Fig. 4A, the inset)			
624[a]	1248	81	$(A1)_6 + A1(O)$
643[a]	1248, 38	70	$(A1)_6 + A1(O,K)$
662[a]	1248, 38 × 2	36	$(A1)_6 + A1(O,K,K)$
712[a]	1248, 176	100	$(A1)_7 + A1(O)$
731[a]	1248, 176, 38	90	$(A1)_7 + A1(O,K)$
750[a]	1248, 176, 38 × 2	58	$(A1)_7 + A1(O,K,K)$
800[a]	1248, 176 × 2	60	$(A1)_8 + A1(O)$
819[a]	1248, 176 × 2, 38	67	$(A1)_8 + A1(O,K)$
838[a]	1248, 176 × 2, 38 × 2	47	$(A1)_8 + A1(O,K,K)$
MS/MS of *m/z* 712 (Fig. 4B–D)			
113	44 × 3, −18	15	$(Q)_3 - H_2O$
131	44 × 3	28	$(Q)_3$
175	44 × 4	100	A1 [=Q × 4]
193	44 × 4, 18	27	$A1 + H_2O$
351	44 × 8	58	$(A1)_2$

[a] Doubly charged ions.

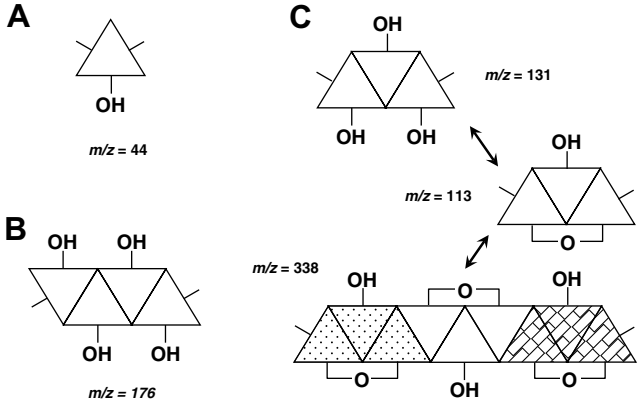

Fig. 4. Schematic representation of the Q (A), A1 (B), and A2 modules (C). Triangles indicate the backbone of the Q module, and available double bonds in the Q module are shown as solid lines from the triangles. The A2 module at *m/z* 338 would be formed by trimerization of the dehydrated tri-Q polymer at *m/z* 113.

basically, since we also observed the 44-Da inter-peak spacing in the FAB-MS spectrum. The molecular structure of the P sample would be much more complicated than that of the B sample.

Dialysis against water using a membrane of MWCO 10000 (Pierce Chemical, Rockford, IL) brought on little loss of the B and P samples (data not shown); therefore, these samples would form considerable large aggregates of the M module. This is one reason why the solid-state

NMR instead of solution NMR was used for the samples. The M modules of the B sample might associate each other mainly by hydrogen bonding, resulting in the formation of such a macromolecule. With regard to hydrogen bonds, Taylor and Kennard (1982) reported interesting evidence based on a survey of 113 published crystal structures that have been determined very precisely by neutron diffraction. In the report, they concluded that the majority of short C–H···O, C–H···N, and C–H···Cl contacts are attractive interactions that can be reasonably described as hydrogen bonds. Therefore, in our case, such hydrogen bonds of C–H···O(H)–C, C–H···O(C)–C, and C–H···N might exist in the aggregates. This is consistent with the solid-state NMR data (Fig. 1C).

The B and P samples have inhibitory activities against several proteinases, and the optimal pH was around 5, indicating that the inhibitory activities depend on the molecular shape or electrostatic potential (Hatano, 2006). Accordingly, it is conceivable that some of the hydrogen bonds are involved in the inhibitory activity, since the hydrogen bonds play an important role for the aggregation of the M modules. In the near future, we plan to investigate the molecular shapes of the B and P samples in detail by light scattering, which would contribute to even better understanding of the mechanisms of the molecular formation and proteinase inhibition.

Acknowledgements

We first wish to thank Dr. Noriko Kagi (JASCO International, Japan) for the use of a Micromass Q-Tof II spectrometer with the Nanoflow ESI interface and for her analytical and technical support. The authors are grateful to Dr. Jun Ashida (Varian Technologies Japan Ltd., Japan) for the use of a Varian Unity INOVA 400WB spectrometer. Drs. Kimihiro Goto (Sumika Chemical Analysis Service) and Koji Nagata (University of Tokyo, Japan) are also appreciated in the elemental analyses and FAB-MS measurements, respectively. This work was supported in part by the NISSAN SCIENCE FUNDATION program to K.-i.H.

References

Aiken, G. R., McKnight, D. M., Wershaw, R. L., & MacCarthy, P. (1985). In G. R. Aiken, D. M. McKnight, R. L. Wershaw, & P. MacCarthy (Eds.), *Humic substances in soil, sediment and water* (pp. 1–9). New York: John Wiley and Sons.

Bennett, A. E., Rienstra, C. M., Auger, M., Lakshmi, K. V., & Griffin, R. G. (1995). Heteronuclear decoupling in rotating solids. *Journal of Chemical Physics, 103*, 6951–6958.

Bielecki, A., Burum, D. P., Rice, D. M., & Karasz, F. E. (1991). Solid-state two-dimensional ^{13}C–^{1}H correlation NMR spectrum of amorphous poly(2,6-dimethyl-*p*-phenylene oxide). *Macromolecules, 24*, 4820–4822.

Hatano, K.-i. (2006). Purification and characterization of novel proteinase inhibitors from dried figs. *Journal of Agriculture and Food Chemistry, 54*, 562–567.

Hayes, M. H. B., MacCarthy, P., Malcolm, R. L., & Swift, R. S. (1989). In M. H. B. Hayes, P. MacCarthy, R. L. Malcolm, & R. S. Swift (Eds.), *Humic substances II. In search of structure* (pp. 3–31). New York: John Wiley and Sons.

Leenheer, J. A., Rostad, C. E., Gates, P. M., Furlong, E. T., & Ferrer, I. (2001). Molecular resolution and fragmentation of fulvic acid by electrospray ionization/multistage tandem mass spectrometry. *Analytical Chemistry, 73*, 1461–1471.

Peersen, O. B., Wu, X. L., Kustanovich, I., & Smith, S. O. (1993). Variable-amplitude cross-polarization MAS NMR. *Journal of Magnetic Resonance, 104A*, 334–339.

Plancque, G., Amekraz, B., Moulin, V., Toulhoat, P., & Moulin, C. (2001). Molecular structure of fulvic acids by electrospray with quadrupole time-of-flight mass spectrometry. *Rapid Communications in Mass Spectrometry, 15*, 827–835.

Reemtsma, T., & These, A. (2003). On-line coupling of size exclusion chromatography with electrospray ionization-tandem mass spectrometry for the analysis of aquatic fulvic and humic acids. *Analytical Chemistry, 75*, 1500–1507.

Stevenson, F. J. (1985). In G. R. Aiken, D. M. McKnight, R. L. Wershaw, & P. MacCarthy (Eds.), *Humic substances in soil, sediment and water* (pp. 13–35). New York: John Wiley and Sons.

Taylor, R., & Kennard, O. (1982). Crystallographic evidence for the existence of C–H···O, C–H···N, and C–H···Cl hydrogen bonds. *Journal of the American Chemical Society, 104*, 5063–5070.

Thurman, E. M. (1985). *Organic geochemistry of natural waters*. Dordrecht: Martinus Nijhoff/Dr. W. Junk Publishers (pp. 280–288).

Vinson, J. A., Zubik, L., Bose, P., Samman, N., & Proch, J. (2005). Dried fruits: excellent *in vitro* and *in vivo* antioxidants. *Journal of the American College of Nutrition, 24*, 44–50.

Wagner, G., Pardi, A., & Wüthrich, K. (1983). Hydrogen bond length and ^{1}H NMR Chemical shifts in proteins. *Journal of the American Chemical Society, 105*, 5948–5949.